Impact of anisotropic diffusion and drifts on cosmic-ray acceleration

Downloaded from: https://research.chalmers.se, 2026-02-16 14:55 UTC

Citation for the original published paper (version of record):
Merten, L., Aerdker, S., Tjus, J. (2025). Impact of anisotropic diffusion and drifts on cosmic-ray acceleration. Proceedings of Science, 501. http://dx.doi.org/10.22323/1.501.0091

N.B. When citing this work, cite the original published paper.

research.chalmers.se offers the possibility of retrieving research publications produced at Chalmers University of Technology. It covers all kind of research output: articles, dissertations, conference papers, reports etc. since 2004. research.chalmers.se is administrated and maintained by Chalmers Library

(article starts on next page)

PROCEEDINGS OF SCIENCE

Impact of anisotropic diffusion and drifts on cosmic-ray acceleration

L. Merten,[1,2,*] **S. Aerdker**[1,2] **and J. Becker Tjus**[1,2,3]

[1]*Theoretical Physics IV, Faculty for Physics & Astronomy, Ruhr University Bochum, Germany*

[2]*Ruhr Astroparticle and Plasma Physics Center (RAPP Center), Germany*

[4]*Department of Space, Earth and Environment, Chalmers University of Technology, Gothenburg Sweden*

Although for classical models of diffusive shock acceleration (DSA) at supernova remnants (SNRs) it is hard to reach PeV energies, SNRs are still believed to contribute a large amount of the total Galactic cosmic-ray luminosity. Nowadays it is clear that SNRs show a significant temporal evolution of those parameters relevant for the transport and acceleration of CRs within and the escape from them; the magnetic field for example can change from being mainly radial to tangential with increasing age of the SNRs. Thus, for an accurate description of CR acceleration over the lifetime of the source, time-dependent models are required, dropping the assumption of parallel shocks. At regions where the shock is oblique, drifts of CRs have to be taken into account. In the case of strong external magnetic fields, such as at SN 1006, the situation becomes even more interesting, drifts potentially drive CRs to regions where the shock is parallel and where DSA is most efficient.

We utilize a new generalized stochastic differential equation solver based on the open source propagation framework CRPropa to model time-dependent DSA in such potential Galactic cosmic-ray sources. We present models of DSA ranging from parallel to perpendicular spherical SNRs, including complex magnetic background fields. Furthermore, we consider anisotropic diffusion which allows CRs to cross magnetic field lines, facilitating DSA at almost perpendicular shocks at which otherwise shock drift acceleration takes over.

The 39th International Cosmic Ray Conference (ICRC2025)
15–24 July, 2025
Geneva, Switzerland

*Speaker

© Copyright owned by the author(s) under the terms of the Creative Commons Attribution-NonCommercial-NoDerivatives 4.0 International License (CC BY-NC-ND 4.0).

PoS(ICRC2025)091

1. Introduction

The increasing observational precision reached for measurements of cosmic ray (CR) acceleration sites such as supernova remnants (SNRs) calls for an improved modeling of the underlying processes. Here, we will take first steps in the direction of a more complete picture of diffusive shock acceleration (DSA) at SNRs. We will examine how different drifts, originating from curvature and gradients in the magnetic field and potentially induced electric fields alter the transport and acceleration of CR. The motion of the Alfvén waves with respect to the plasma background flow form another source of drifts that can effectively change the compression ratio of the shock seen by the CRs; leading to deviation from the canonically expected spectral index γ of the energy spectrum.

First, we will describe the methods to solve the transport equation in sec. 2 in general and derive the relevant drift terms for the readers convenience in sec. 3. After that we will discuss the influence of the drifts on the spatial distribution (sec. 4) and the energy spectrum (sec. 5).

2. Methods

CR transport and acceleration is modeled with a modified version of CRPropa 3.2 [1] with an updated structure for the solution of stochastic differential equations (SDEs) [3]. A brief overview of diffusive particle transport with SDEs is given in the following with a focus on the newly implemented drift terms, allowing to take spatial dependent eigenvalues of the diffusion tensor and additional drifts due to the magnetic field structure into account. While CRPropa was originally designed for Monte Carlo simulations of ultra-high energy CRs, the ensemble-averaged approach introduced by [4] extended the CRPropa framework to Galactic transport. In this macroscopic description, assuming an isotropic distribution in momentum p, the time evolution of the distribution function f can be described by the transport equation

$$\frac{\partial f}{\partial t} = \nabla \cdot (\hat{\kappa} \nabla f - \mathbf{v} f) - \mathbf{w} \cdot \nabla f + \frac{p}{3} \nabla \cdot \mathbf{w} \frac{\partial f}{\partial p} + \frac{1}{p^2} \left(\frac{\partial}{\partial p} p^2 D_{pp} \frac{\partial f}{\partial p} \right) - Lf + S \quad , \tag{1}$$

where $\hat{\kappa}$ encodes the spatial diffusion in the presence of turbulent magnetic fields, $\mathbf{u} = \mathbf{v} + \mathbf{w}$, with $\mathbf{w} = -\nabla\phi$, $\mathbf{v} = \nabla \times A$, the advection with the background plasma and S any sources and sinks. In the local frame of the magnetic field line diagonal entries of $\hat{\kappa}$ denote diffusion parallel/perpendicular to the magnetic field; off-diagonal entries represent drifts due to gradient and curvature of the magnetic field (e.g. [6]). Equation 1 can be re-written into a Fokker-Planck form by introducing the differential number density $\mathcal{N} = p^2 f$.

$$\frac{\partial \mathcal{N}}{\partial t} = \frac{1}{2} \nabla^2 (2\hat{\kappa}\mathcal{N}) - \nabla \left[(\nabla \hat{\kappa} + \mathbf{u}) \mathcal{N} \right] - \frac{\partial}{\partial p} \left[-\frac{p}{3} (\nabla \cdot \mathbf{u}) \mathcal{N} \right] + S \quad , \tag{2}$$

where momentum diffusion, as it is not discussed in this work, has been neglected ($D_{pp} = 0$). Any Fokker-Planck equation is equivalent to a set of SDEs, so that eq. (2) can be translated to

$$\mathrm{d}\mathbf{x} = (\mathbf{u} + \nabla \cdot \hat{\kappa}) \, \mathrm{d}t + \sqrt{2\hat{\kappa}} \mathrm{d}\mathbf{W}_t \quad , \quad \mathrm{d}p = -\frac{p}{3} \nabla \cdot \mathbf{u} \mathrm{d}t \quad , \tag{3}$$

PoS(ICRC2025)091

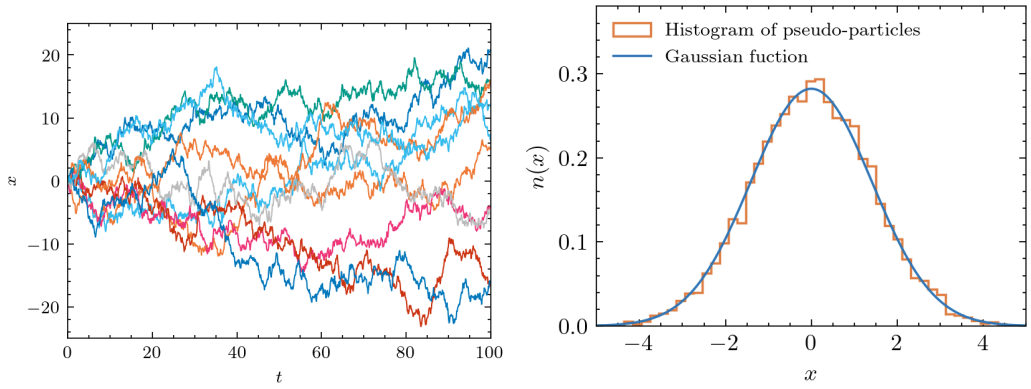

Figure 1: Exemplary pseudo-particle trajectories, solutions of the purely diffusive SDE $\mathrm{d}x = \kappa \mathrm{d}W_t$ (left) and corresponding histogram over space, compared to the Gaussian function solving the related transport equation (right). Fig. courtesy by S. Aerdker, orig. PhD dissertation (2025)

where the Wiener process $\mathrm{d}\mathbf{W}_t$ is introduced as a stochastic driver for the spatial diffusion. Without momentum diffusion, changes in momentum are given by an ordinary differential equation. The solutions of eq. (3) *sample* the differential number density $\mathcal{N}$ and are called *pseudo-particles* in the following. By integrating many instances of eq. (3) the macroscopic quantity $\mathcal{N}$ can be recovered. Figure 1 shows pseudo-particle trajectories of the one-dimensional purely diffusive SDE $\mathrm{d}x = \kappa \mathrm{d}W_t$ and the corresponding distribution function, which is a Gaussian function. In this macroscopic picture, DSA results from the interplay of diffusion and adiabatic heating due to the diverging advection $\mathbf{u}$ at the shock.

2.1 Integrating stochastic differential equations

The SDE eq. (3) is integrated with an Euler-Maruyama scheme, an extension of the well-known Euler scheme where the quantity y is subject to Gaussian noise

$$y_{i,n+1} = y_{i,n} + A_i(y_n, t_n)\Delta t + B_{i,j}(y_n, t_n)\Delta W_{i,n} \quad . \tag{4}$$

Here, the components A_i correspond to the drift-like terms of the Fokker-Planck equation, B represents the diffusive terms where $B_{ij} = \delta_{ij}\sqrt{2\kappa_{ij}}$ in the frame of the magnetic field line. The Wiener process is approximated by $\Delta W_n = W(t_{n+1}) - W(t_n)$; Gaussian distributed random numbers with a mean value of zero and variance of the time step Δt. In general, the Euler-Maruyama scheme converges with strong order of $1/2$ and weak order of 1. The weak order is sufficient when the spatial distribution of particles is of interest. However, when modeling shock acceleration the strong order of convergence becomes important, since pseudo-particles have to encounter the region of diverging advection (see [5] for details, especially resulting in constraints on the time step). In case of additive noise, that is for spatially constant diffusion coefficients, the strong order of convergence becomes also equal to 1 [7]. In case of strong drifts due to a sudden change of the spatial diffusion coefficient at the shock, higher-order schemes, e.g. a predictor-corrector scheme, should be used instead (see [8]).

Note that, when diffusion in momentum is not considered, the change in momentum is deterministic but depends on the stochastic movement of particles leading to a correlated one-sided

PoS(ICRC2025)091

random walk.

Solving for the differential number density applying stochastic differential equations has been shown to be a fast and flexible method in the past. For the investigation of DSA at blast waves, time-dependent advection fields were added to the modified CRPropa version.[1] Furthermore, anomalous diffusion can be taken into account by exchanging the stochastic driver of the SDE, i.e. the Wiener process to a Lévy process as done in [9] [10]. Here, we present a new extension, considering additional drift terms corresponding to the off-diagonal entries of the diffusion tensor $\hat{\kappa}$, drifts due to electric fields, as well as drifts due to the net motion of magnetic turbulence.

3. Drifts

With drifts we refer to those deterministic motions of the particle ensemble f (or $\mathcal{N}$) that are not included in the original plasma flow $\mathbf{u}$; examples for such drifts are the curvature and gradient drifts of the magnetic field summarized as

$$\mathbf{v}_d = \frac{pvc}{3qB^4}\left(B^2\left(\nabla\times\mathbf{B}\right) + B\times\nabla B^2\right) = \frac{pvc}{3q}\left(\nabla\times\frac{\mathbf{B}}{B^2}\right) \quad , \tag{5}$$

where $\mathbf{B}$ is the magnetic field, p is the absolute particle momentum, v its speed and q its charge. In the presence of electric fields, the E-cross-B drift

$$\mathbf{v}_E = \frac{\mathbf{E}\times\mathbf{B}}{B^2} = -\frac{(\mathbf{v}\times\mathbf{B})\times\mathbf{B}}{B^2} \quad , \tag{6}$$

where we used the assumptions of ideal MHD equations for the electric field $\mathbf{E} = -\mathbf{v}\times\mathbf{B}$ occurs, too. It directly becomes clear that $\nabla\cdot\mathbf{v}_d = 0$, meaning that the curvature and gradient drifts do not work on the particles, keeping their energy unchanged. However, some acceleration sites provide environments such that $\mathbf{E}\cdot\mathbf{v}_d \neq 0$, so particles can drift along the electric field and gain energy. In the single particle picture at quasi-perpendicular shocks, this effect is usually referred to as *shock drift acceleration*.

Furthermore, particles are isotropized with respect to the frame that moves with the scatter centers (e.g. [11]). It has been suggested that the movement of such scatter centers, i.e. the local velocity of magnetic waves v_w, cannot always be neglected with respect to the motion of the fluid u [12]. Unlike drifts due to curvature and gradient of the magnetic field, the drift v_w is, in general, not divergence free and, thus, can change the *effective* compression ratio of the shock, contributing to particle energization.

We will first, discuss the implementation and present test cases focusing on the spatial displacement of the particle distribution. Then, we present effects on the energy spectrum and discuss how stochastic models can be used to model an interplay of shock drift acceleration and spatial diffusion, similar to the stochastic shock drift acceleration models by [13].

[1] Time-dependent advection fields will become publicly available in the master version of CRPropa soon and are introduced in another contribution, *CRPropa 3.3: Toward a Unified Multi-Messenger Framework from GeV to ZeV Energies.*

PoS(ICRC2025)091

4. Spatial displacement

4.1 Planar shock

For a planar oblique shock where the magnetic field **B** intersects the plasma flow **u** under an angle α (see Fig. 2) the drift velocity due to curvature and gradient drifts can be calculated. Keeping in mind, that the drift must be calculated as an *averaged* property[2] the drift is given by

$$\begin{aligned}\bar{\mathbf{v}}_d &= \frac{1}{L_z L_x}\int \mathbf{v}_d \,\mathrm{d}\mathbf{S} = \frac{pvc}{3ZeL_zL_x}\int \epsilon_{ijk}\frac{\partial}{\partial x_j}\frac{B_k}{B^2}\,\mathrm{d}S_i = \frac{pvc}{3ZeL_zL_x}\oint_C \frac{B_i}{B^2}\,\mathrm{d}r_i \\ &= \frac{pvc}{3ZeLB}\left[\frac{q-(\cos^2(\alpha)+\sin^2(\alpha)q^2)}{\cos^2(\alpha)+\sin^2(\alpha)q^2}\sin(\alpha)\right] \quad . \end{aligned} \tag{7}$$

Here, ϵ_{ijk} is the totally anti-symmetric Levi-Cevita tensor and Stoke's theorem was used to transform from an area integration to a closed line integral. To derive the final result we used that the magnetic field component perpendicular to the shock normal is increased by the compression ratio q; $B_{2,z} = qB_{1,z}$ while the parallel component is unchanged $B_{2,x} = B_{1,x}$ (see also [6]).

The direction of the drift changes with the inclination angle α, meaning that particle drift along or anti-parallel to the electric field, depending on the obliquity. The drift vanishes outside a small region around the shock for $|x - x_{sh}| > L$, as the magnetic field is constant on either site of the shock and therefore no drifts occur. The length scale L is usually associated with the gyro radius of the particle.

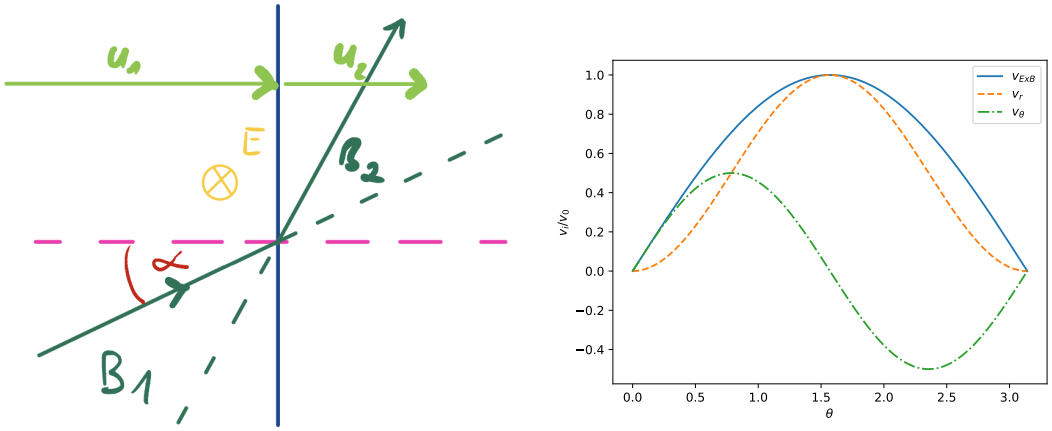

Figure 2: Left: Oblique shock with an electric field E that is induced into the plane of drawing, because the plasma flow u is not parallel to the magnetic field B. Gradient and curvature drifts (see eq. 7) are parallel to the electric field. **Right:** Normalized drift velocity in spherical coordinates.

4.2 Spherical termination shock

A SNR's wind profile can — in a rough estimate — be approximated as a spherical termination shock. When the background magnetic field into which the SNR is expanding is strong, we might assume that it is unaltered, leading to variable obliquity, depending on the latitude θ[3].

[2] In this example we average over an rectangular area perpendicular to the drift velocity v_d with lengths L_x and L_z

[3] We choose the coordinate system in such a way that $\mathbf{B} = B_0\mathbf{e}_z$.

PoS(ICRC2025)091

We assume a termination shock with a shock radius $r_{sh} = 5\,\mathrm{pc}$ that has an upstream velocity of $\mathbf{v}_1 = 3000\,\mathrm{km\,s^{-1}}$, which drops at the shock with a compression ratio of $q = 4$ and continues with a decreasing speed on the downstream site $v(r > r_{sh}) \propto r^{-2}$. The flow speed $\mathbf{v}(\mathbf{r}) = v(r)\mathbf{e}_r$ is in radial direction and the magnetic field is oriented along the cartesian z axis ($\mathbf{B} = B_0\mathbf{e}_z$).

This leads to an electric field $\mathbf{E} = v(r)\sin(\theta)\mathbf{e}_\phi$ and a drift velocity $\mathbf{v}_E = v(r)\sin(\theta)(\cos(\theta)\mathbf{e}_\theta + \sin(\theta)\mathbf{e}_r)$. So the particles will drift faster away from the shock and also drift from the equator to the poles. Figure 2 (right) shows the drift velocities components normalized to the local plasma flow speed in dependence of the latitude θ.

We ran simulation with and without the inclusion of the drift term and for purely parallel to the background magnetic field and isotropic diffusion. Injecting particles slightly upstream of the shock at $r = 4.75\,\mathrm{pc}$ and following $N = 10^6$ initial pseudo-particles for a total time of 300 years, taking 1000 snap shots to model the time evolution.

Figure 3 shows the number density of cosmic rays at $t = 184\,\mathrm{yr}$ after their injection in the upstream region for the case of anisotropic diffusion and including the E-cross-B drift. It can be clearly seen that the particle are propagating faster in at the equator but diffuse only along the magnetic field. At this point in time, particle acceleration is strongest for medium latitudes as they get there quicker than to the poles.

Comparing the influence of anisotropic diffusion and the E-cross-B drift we find that the anisotropy of the diffusion tensor plays the more important role in this specific set-up. Including drift, however, emphasizes the effects of anisotropic/parallel diffusion (see Fig. 4).

5. Energy spectrum

5.1 Changing the effective compression ratio

The test particle approach we show in this proceedings does not capture any interactions between CRs and the background plasma. However, when CRs carry a fraction of the shock's energy that is non-negligible, they cannot be treated as test particles anymore. Such non-linear theory of DSA predicts a *precursor* forming before the shock, effectively increasing the total compression ratio of the shock (e.g. [14]. On the other hand, hybrid simulations show the formation of a *postcursor* due to more efficient advection downstream of the shock [12]. The effect of both can be taken into account approximately with our approach as well, when the advection field u is e.g. informed by hybrid simulations.

Here, we show that we obtain steeper spectra at the shock, when the compression ratio is reduced due the motion of magnetic structures in the downstream region with respect to mean motion of the plasma u. This drift is comparable to the Alfvén speed, such that the compression ratio R is altered [12]

$$\tilde{R} = \frac{u_1}{u_2 + v_{\mathrm{A},2}} = \frac{R}{1+\alpha} \quad , \quad \alpha = \frac{v_{\mathrm{A},2}}{u_2} \quad , \tag{8}$$

where the parameter α is determined by the magnetic pressure ξ_B and the original compression ratio R: $\alpha = \sqrt{2\xi_\mathrm{B}R}$. Note, that the compression ratio R seen by high-energy particles can be higher than 4 when a precursor is considered.

Figure 3 (right) shows the time evolution of the energy spectrum at a planar shock with an effective compression ratio $\tilde{R} = 2.5$ and constant diffusion coefficient. The spectrum is steeper and

PoS(ICRC2025)091

matches the expected spectral slope

$$s = \frac{\tilde{R}+2}{\tilde{R}-1} \quad , \tag{9}$$

which, for $\tilde{R} = 2.5$ becomes E^{-3}. In the future, energy-dependent diffusion together with a spatial structure of the postcursor/precursor can be treated, leading to a more complex spectral shape, depending on the particles' energy and the effective compression ratio they probe.

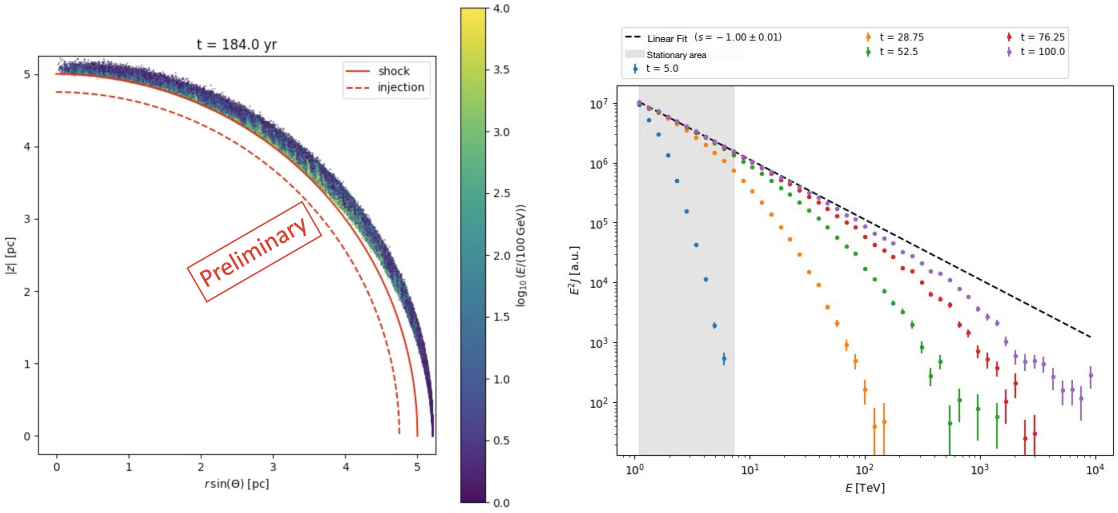

Figure 3: Left: Distribution of CRs after their propagation to the shock and successive DSA their. The shown model is for anisotropic diffusion along the z-direction and includes the E-cross-B drift. **Right:** Time evolution of the energy spectrum at a 1D planar shock with effective compression ratio $\tilde{R} = 2.5$. Particles are continuously injected with energy E_0. The spectrum is fitted at $t = 100$ in the energy region where the stationary solution is reached (indicated by the gray area).

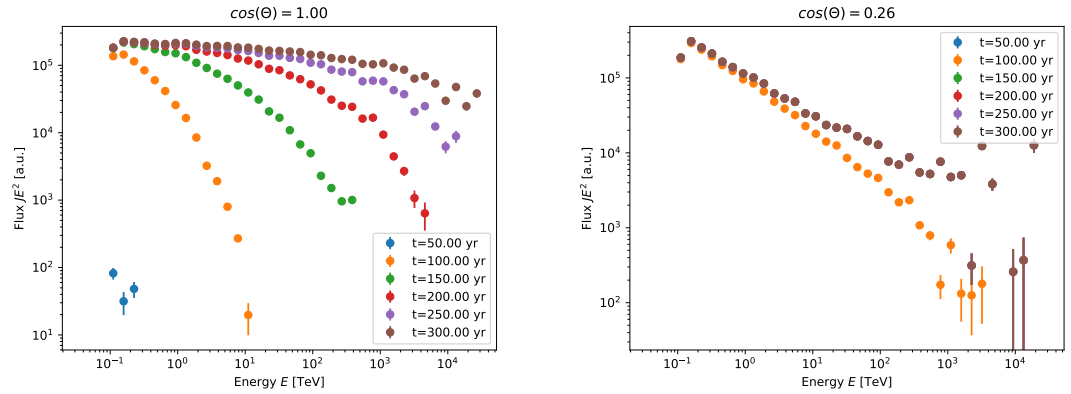

Figure 4: Time evolution of the energy spectra for anisotropic diffusion ($\kappa_\perp = 0$). Here, the effect of the E-cross-B drift is neglected. **Left:** Energy spectra at the poles reach the expected spectral index of $\gamma = -2$. **Right:** This is not true for latitude closer to the equator, because particles are no longer diffusing efficiently back over the shock.

PoS(ICRC2025)091

6. Summary and Outlook

We have shown that the anisotropy of cosmic ray transport can play an important role for the acceleration of CRs at SNR. Drifts induced by curvature or gradients in the magnetic field can emphasize this effect. In cases where magnetic field and flow velocity are not aligned an electric field is induced and additional acceleration of the particle due to drifts along the magnetic field can occur. Here, we focused on the influence that the drifts have on the transport of the particles. Future work will also take the shock drift acceleration in the ensemble averaged picture into account, as already suggested by Jokipii. We do not expect large changes to the overall spectrum but rather a small boost especially at early times.

Furthermore, we have outlined a procedure to take the effect of non-linear feedback of the CRs on the scattering centers, forming a pre-/ or postcursor, into account. This non-linear approach cannot be modeled with the SDE approach of CRPropa alone but needs the information of hybrid simulations.

Acknowledgements

LM, SA, and JT acknowledge support from the Deutsche Forschungsgemeinschaft (DFG): this work was performed in the context of the DFG-funded Collaborative Research Center SFB1491 "Cosmic Interacting Matters - From Source to Signal", project no. 445052434.

References

[1] R. Alves Batista et al. JCAP **09** (2022) 035
[2] L. Merten et al. JCAP **06** (2017) 0 46
[3] L. Merten and S. Aerdker CCP **311** (2025) 109542
[4] L. Merten, et al. JCAP, Issue 06, id. 046 (2017)
[5] S. Aerdker, et al. JCAP, Issue 01, id. 068 (2024)
[6] J. R. Jokipii APJ, 1, vol. 255 (1982)
[7] P. E. Kloeden, and E. Platen. Springer (1992)
[8] A. Achterberg and K. M. Schure MNRAS, Vol. 411, Issue 4 (2011)
[9] F. Effenberger, et al. A&A, Vol. 686, id.A219 (2024)
[10] S. Aerdker, et al. A&A, Vol. 693, id.A15 (2025)
[11] R. Schlickeiser APJ, vol. 336 (1989)
[12] D. Caprioli, C. Haggerty, P. Blasi APJ, Vol. 905, 1, id.2, (2020)
[13] T. Katou and T. Amano APJ Vol. 874, 2, id. 119 (2019)
[14] E. Amato and P. Blasi MNRAS Letters, Vol. 364, 1 (2005)

PoS(ICRC2025)091